Iterative Pre-Compensation of I/Q Imbalances in an Adaptive 2.4 GHz MIMO-OFDM System

M. Petermann, M. Niemiec, D. Wübben, K.-D. Kammeyer
Department of Communications Engineering
University of Bremen, 28359 Bremen, Germany
Email: petermann@ant.uni-bremen.de

M. Stefer, M. Schneider
RF & Microwave Engineering Laboratory
University of Bremen, 28359 Bremen, Germany
Email: markus.stefer@hf.uni-bremen.de

***Abstract*—Currently evolving communication standards, especially those using multi-antenna (MIMO) multicarrier modulation techniques, are based on the exploitation of channel state information (CSI) at the transmitter. The utilization of adaptive transmission schemes comes with a more sensitive behavior with respect to front-end imperfections. Direct-conversion architectures in turn allow for low-cost transceiver solutions but introduce higher imbalances of the in-phase (I) and quadrature (Q) branches. For adaptive systems with high data rates severe performance losses are observed with respect to bit error rates (BER). In this paper the influence of transmitter side I/Q imbalances is investigated with respect to a MIMO hardware demonstrator, which applies adaptive Orthogonal Frequency Division Multiplexing (OFDM) strategies. An enhanced algorithm for blind online pre-compensation is presented. Comparable single-tone low-IF measurement results indicate an improved image signal suppression and higher convergence robustness while the system shows decreased downlink BER after compensation.**

I. Introduction

Future wireless communication systems will require multi-mode standard terminals that support existing air interface technologies like Orthogonal Frequency Division Multiplexing (OFDM) as well as evolving wireless transmission schemes [1]. Additionally, these systems should employ higher bandwidths, higher modulation constellation orders and multiple-input multiple-output (MIMO) principles. As a consequence, the systems become more sensitive to front-end non-idealities like inphase (I) and quadrature (Q) gain and phase imbalances. Hence, the demand for flexible low-cost analogue front-ends with low power consumption will increase dramatically [1], [2]. This is substantiated by the fact that multi-antenna systems need multiple front-ends with possible component variations.

One possible low-cost front-end mixing concept is the so-called zero-IF or direct-conversion principle since it does not require intermediate frequencies (IF) and image rejection filters. Thus, it allows for low-cost solutions via monolithic integration of the analogue front-ends [3], [4]. In contrast, this direct conversion causes gain and phase imbalances in the mixing branches. The sensitivity to these imbalances at the transmitter (Tx) side is even more obvious in adaptive communication systems, where Tx pre-processing is applied to adapt to the current channel condition as well as to reduce the complexity of the mobile terminals in terms of downlink transmission [5]–[7]. To comparably reduce the effort at the mobile terminals spent for compensation of the non-ideal mixing in the transmitter, pre-correction of the I/Q imbalance at the transmitter side is suggested, e.g., in [8], [9]. There are two types of methods for pre-correction of I/Q imbalances, which can be distinguished between offline and online calibration schemes [9]. Some offline algorithms based on calibration signals measuring the radio frequency (RF) response at the transmitter are shown in [10]–[13]. Online algorithms for pre-compensation are achieved, e.g., by detecting the RF envelope power as in [8], while an adaptive algorithm based on RF feedback is suggested in [14].

Furthermore, several approaches for estimation and compensation of I/Q imbalance in OFDM systems have been proposed, e.g., in [3], [15], [16]. In [17] the estimation of imbalance parameters at the receiver and a feedback of this parameters to the transmitter is proposed. Unfortunately, this procedure comes with a decrease in effective uplink rate, which ideally should also be avoided. Therefore, a fast algorithm introduced in [18], [19] can be applied, which is working during regular transmission and only needs some hardware modifications at the Tx side to enable a low intermediate-frequency (low-IF) feedback.

In this contribution the influence and compensation of transmit I/Q imbalance in adaptive MIMO-OFDM systems applying either bit and power loading strategies [5], [20] or linear zero-forcing pre-equalization [6] is investigated with the help of a multiple antenna hardware demonstrator. Based on an enhanced pre-compensation algorithm following [19] the existing Tx side I/Q imbalance parameters of the demonstrator front-ends are determined and fed back to adapt the system to the imbalanced situation. After applying this compensation in the Tx baseband processing the resulting bit error rates (BER) are compared to the uncompensated case.

The remainder of the paper is organized as follows. In Section II a general mathematical description of the investigated system is given. While Section II-A deals with the influence of transmit I/Q imbalance, Section II-B introduces the adaptive MIMO-OFDM baseband structure and shows the influence of transmit I/Q imbalance on such systems. The utilized modified iterative pre-compensation algorithm is

This work was supported in part by the German Research Foundation (DFG) under grant KA 841-21/1 and SCHN 1147/2-1.

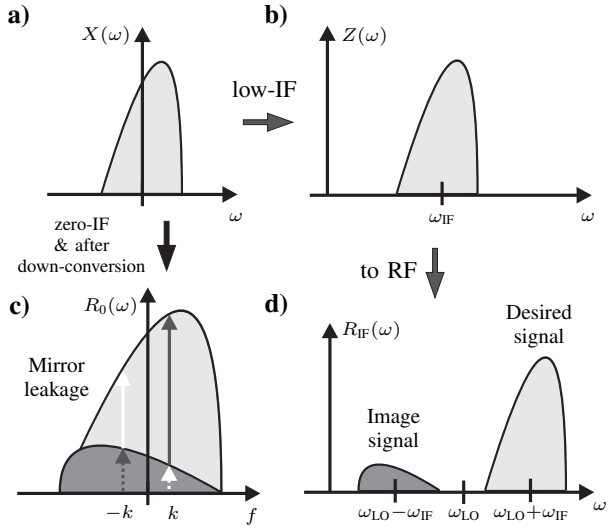

Fig. 1. Signal spectra in a transmitter with I/Q imbalance:
a) Baseband signal; b) IF signal; c) Receive baseband signal of a direct-conversion transceiver with I/Q imbalance, mirror leakage indicated for subcarrier k; d) RF signal of low-IF transmitter with I/Q imbalance

derived in Section III-A, a performance analysis concerning different initial values and quantization effects in the compensation structure is provided accordingly in Section III-B. Applying the multiple antenna demonstrator in Section IV-A, Section IV-C subsequently presents BER measurement results at 2.4 GHz obtained with and without I/Q imbalance compensation. Prior to that, the I/Q imbalance parameters of the individual demonstrator Tx front-end modules needs to be determined in Section IV-B. Finally, Section V draws some conclusions and highlights the main contributions of this paper.

II. System and I/Q Imbalance Model

The following section describes the direct-conversion principle and gives a short insight in the context of transmit I/Q imbalance in the considered MIMO-OFDM system. It is assumed that no receive I/Q imbalance is present at both transceivers, which in general is not the case.

A. I/Q Imbalances

Perfectly balanced I/Q mixing, meaning equal gain and a 90° phase shift between the I and Q branches, is usually not feasible, e.g., due to hardware tolerances. In terms of direct-conversion (or zero-IF) transceivers this leads to (undesired) mirror leakage in the baseband signal. This is illustrated in Fig. 1a) to Fig. 1c). The I/Q imbalances can usually be modeled as phase and amplitude errors in the local oscillator (LO), which is the same as modeling the errors in the signal path [21]. Hence, considering a direct-conversion system with N_B transmit and N_M receive antennas, the signal $\mathbf{x}(t)$ of all N_{B} transmit antennas after D/A conversion is multiplied with an imbalanced LO signal $y_{\text{LO}}(t) = \cos(\omega_{\text{LO}}t) + j \cdot g_T \sin(\omega_{\text{LO}}t + \phi_T)$, where g_T is the gain imbalance and ϕ_T the phase imbalance. ω_{LO} denotes the angular LO frequency. If the mixer is perfectly matched the parameters $g_T = 1$ and $\phi_T = 0$ hold. Without loss of generality *frequency-independent imbalance* is assumed throughout the paper. The transmitted RF signal of transmit antenna n_{B} after up-conversion can be written as [4]

$$\begin{aligned} x_{\text{RF},n_{\text{B}}}(t) &= 2\,\text{Re}\{x_{n_{\text{B}}}(t) y_{\text{LO}}(t)\} && \text{(1a)} \\ &= \left(K_{1,n_{\text{B}}} x_{n_{\text{B}}}(t) + K^*_{2,n_{\text{B}}} x^*_{n_{\text{B}}}(t)\right) \text{e}^{j\omega_{\text{LO}}t} \\ &\quad + \left(K^*_{1,n_{\text{B}}} x^*_{n_{\text{B}}}(t) + K_{2,n_{\text{B}}} x_{n_{\text{B}}}(t)\right) \text{e}^{-j\omega_{\text{LO}}t}, && \text{(1b)} \end{aligned}$$

with coefficients $K_{1,n_{\text{B}}}$ and $K_{2,n_{\text{B}}}$ given by

$$K_{1,n_{\text{B}}} = \frac{1}{2}\left(1 + g_{T,n_{\text{B}}} \text{e}^{+j\phi_{T,n_{\text{B}}}}\right) = \frac{1}{2}\left(1 + \alpha_{n_{\text{B}}} + j\beta_{n_{\text{B}}}\right) \quad \text{(2a)}$$

$$K_{2,n_{\text{B}}} = \frac{1}{2}\left(1 - g_{T,n_{\text{B}}} \text{e}^{-j\phi_{T,n_{\text{B}}}}\right) = \frac{1}{2}\left(1 - \alpha_{n_{\text{B}}} + j\beta_{n_{\text{B}}}\right) \quad \text{(2b)}$$

and the factor 2 added for notational convenience. The perfect matching case again results in parameters

$$\alpha_{n_{\text{B}}} = g_{T,n_{\text{B}}} \cos(\phi_{T,n_{\text{B}}}) = 1 \quad \text{and} \quad \text{(3a)}$$

$$\beta_{n_{\text{B}}} = g_{T,n_{\text{B}}} \sin(\phi_{T,n_{\text{B}}}) = 0\,. \quad \text{(3b)}$$

Equation (1b) shows that the imperfect mixing produces an extra term due to the I/Q imbalance, which causes the overlapping of the original and the mirror spectra in the baseband after down-conversion as in Fig. 1c).

In contrast to the direct-conversion principle, the low-IF scheme provides the digital up-conversion to an intermediate frequency as depicted in Fig. 1a) and Fig. 1b), where now the low-IF signal is multiplied with the LO signal. Regarding the RF signal of such a mixing, the desired and the image signal are split up. Consequently, this allows for determination of the so-called image-to-signal-power ratio (ISR) per transmit antenna, which is independent from the transmit power [19]. An exemplary RF signal is shown in Fig. 1d). The ISR is defined as

$$ISR(\alpha_{n_{\text{B}}}, \beta_{n_{\text{B}}}) = \frac{|K_{2,n_{\text{B}}}|^2}{|K_{1,n_{\text{B}}}|^2} = \frac{(1-\alpha_{n_{\text{B}}})^2 + \beta^2_{n_{\text{B}}}}{(1+\alpha_{n_{\text{B}}})^2 + \beta^2_{n_{\text{B}}}}\,. \quad (4)$$

This definition for a low-IF structure is introduced as it is necessary for the derivation of the pre-compensation algorithm in Section III-A.

B. Adaptive MIMO-OFDM Signal Model

As the influence of I/Q imbalance on adaptive multi-antenna multi-carrier systems shall be investigated, the effects on such systems need to be specified. Therefore, an adaptive OFDM system with N_c subcarriers applying precoding per subcarrier k using a precoding matrix $\mathbf{F}(k) \in \mathbb{C}^{N_{\text{B}} \times N_{\text{M}}}$ is considered such that the receive baseband signal in frequency-domain *without* I/Q imbalance can be written as

$$\mathbf{r}(k) = \mathbf{Z}(k)\mathbf{H}(k)\mathbf{F}(k)\mathbf{d}(k) + \beta^{-1}(k)\tilde{\mathbf{n}}(k) \quad (5)$$

for all subcarriers $k = -N_c/2, \ldots, N_c/2$ but omitting the DC carrier ($k = 0$) to avoid DC offset problems. The vector $\tilde{\mathbf{n}} \in \mathbb{C}^{N_{\text{M}} \times 1}$ is a (post-filtered) white Gaussian noise term, where the same noise power σ_n^2 before filtering on all subcarriers and all receive antennas is assumed. Furthermore,

perfect synchronization and a sufficiently long guard interval is supposed. The data symbols in vector $\mathbf{d}(k) \in \mathbb{C}^{N_\mathrm{M}\times 1}$ are taken from a square M-QAM signal constellation, where here M can be any positive power of two up to 1024, depending on the modulation scheme assigned from, e.g., a bit and power loading algorithm in [5]. Consequently, the transmit data per subcarrier in the baseband is $\mathbf{x}(k) = \mathbf{F}(k)\mathbf{d}(k)$. The scalar

$$\beta(k) = \sqrt{\frac{N_B}{\mathrm{tr}\left\{\mathbf{F}(k)^H\mathbf{F}(k)\right\}}} \tag{6}$$

is defined to fulfill the total sum power constraint per subcarrier. The forward link channel matrix $\mathbf{H}(k) \in \mathbb{C}^{N_\mathrm{M}\times N_\mathrm{B}}$ or an accurate estimate $\hat{\mathbf{H}}(k) \in \mathbb{C}^{N_\mathrm{M}\times N_\mathrm{B}}$ must be known to the transmitter to enable the precoding. In order to correct estimation and phase errors at the receiver linear post-filtering with matrix $\mathbf{Z}(k) \in \mathbb{C}^{N_\mathrm{M}\times N_\mathrm{M}}$ is realized [20], [22].

In this paper, two different cases of pre- and post-processing with matrices $\mathbf{F}(k)$ and $\mathbf{Z}(k)$ are distinguished for the measurements in Section IV:

Case I) In a point-to-point communication system all data is transmitted to a single user. The estimated channel matrix can be decomposed into $\hat{\mathbf{H}}(k) = \mathbf{U}(k)\mathbf{\Sigma}(k)\mathbf{V}^H(k)$ via singular value decomposition (SVD) to obtain N_B parallel single-input single-output (SISO) channels per subcarrier. Then, the pre-processing matrix is $\mathbf{F}(k) = \mathbf{V}(k)$ and the post-processing matrix results in $\mathbf{Z}(k) = \hat{\mathbf{H}}_{\text{eff}}^{+}(k)$ with the pseudo-inverse $(\cdot)^+$ of the effective channel matrix $\hat{\mathbf{H}}_{\text{eff}}(k) = \mathbf{H}(k)\mathbf{V}(k)$ that needs to be estimated at the receiver. After parallelization of the subchannels a bit and power loading algorithm is used based on [5].

Case II) In a point-to-multipoint communication the precoding intends to suppress the interference of the individual receiver data prior to the transmission. Therefore, a common method is to use the pseudo-inverse of $\mathbf{H}(k)$ for pre-processing such that $\mathbf{F}(k) = \hat{\mathbf{H}}^{+}(k)$. If there exist some errors in the channel estimate, the post-processing needs to account for those errors by applying $\mathbf{Z}(k) = \mathrm{dg}\left\{\hat{\mathbf{H}}_{\text{eff}}(k)\right\}^{-1}$ for the non-cooperative receivers with the estimated effective channel matrix $\hat{\mathbf{H}}_{\text{eff}}(k) = \mathbf{H}(k)\mathbf{F}(k)$. The operator $\mathrm{dg}\{\cdot\}$ sets all off-diagonals of a matrix to zero.

To include the I/Q imbalance model, with the assumption of ideal down-conversion at the receiver the time-domain signal after inverse discrete Fourier transform (IDFT) is $\hat{\mathbf{x}}(t) = \mathbf{K}_1\mathbf{x}(t) + \mathbf{K}_2^*\mathbf{x}^*(t)$ [21]. Taking (1b) into account, (5) can be written as

$$\begin{aligned}\mathbf{r}(k) &= \mathbf{Z}(k)\mathbf{H}(k)\left[\mathbf{K}_1\mathbf{x}(k) + \mathbf{K}_2^*\mathbf{x}^*(-k)\right] \\ &= \mathbf{Z}(k)\mathbf{H}(k)\mathbf{K}_1\mathbf{x}(k) + \mathbf{Z}(k)\mathbf{H}(k)\mathbf{K}_2^*\mathbf{x}^*(-k)\,, \end{aligned} \tag{7}$$

where the noise term has been neglected for brevity. The imbalance matrices according to (2) are defined as diagonal matrices

$$\mathbf{K}_1 = \frac{1}{2}\left(\mathbf{I}_{N_B} + \mathbf{G}_T\mathrm{e}^{+j\mathbf{\Phi}_T}\right) \tag{8a}$$

$$\mathbf{K}_2 = \frac{1}{2}\left(\mathbf{I}_{N_B} - \mathbf{G}_T\mathrm{e}^{-j\mathbf{\Phi}_T}\right)\,. \tag{8b}$$

In (8a) and (8b) the gain and phase imbalance parameters of all transmit antennas are covered by the matrices

$$\mathbf{G}_T = \mathrm{diag}\left\{g_{T,1}, \ldots, g_{T,n_\mathrm{B}}\right\} \tag{9a}$$

$$\mathbf{\Phi}_T = \mathrm{diag}\left\{\phi_{T,1}, \ldots, \phi_{T,n_\mathrm{B}}\right\}\,, \tag{9b}$$

where the $\mathrm{diag}\{\cdot\}$-operator sets up the elements of a vector on the diagonals of a matrix. The system equation in (7) indicates the intercarrier-interference (ICI) due to I/Q imbalances caused by the overlapping of mirror subcarriers $-k$ and k, which is also highlighted in Fig. 1c).

III. I/Q Imbalance Tx Pre-Compensation

In this section an applicable I/Q imbalance pre-compensation algorithm is introduced by a short repetition of the scheme in [19], which forms the basis for the iterative scheme used here. In addition, the considered algorithm is modified and a convergence analysis is given to prove the efficiency.

A. Modified Iterative Pre-Compensation Algorithm

The selected algorithm in [19] is based on blind estimation of the parameters α_{n_B} and β_{n_B} during regular transmission. Therefore, it is necessary to establish a hardware feedback loop at the transmitter, which down-converts the RF signal to an intermediate frequency (IF) [19]. This avoids additional I/Q imbalance in this feedback path. Hence, the desired signal and the image signal are split up to the frequencies $\omega_\mathrm{LO} + \omega_\mathrm{IF}$ and $\omega_\mathrm{LO} - \omega_\mathrm{IF}$ as in Fig. 1d), which enables ISR measurements based on the estimated parameters $\hat{\alpha}_{n_\mathrm{B}}$ and $\hat{\beta}_{n_\mathrm{B}}$.

For the upcoming analysis the algorithm in [19] is restated, which is called Windisch's algorithm in the following. This algorithm uses the assumption, that the I/Q imbalance can be represented by one virtual I/Q imbalance model with resulting parameters (antenna index is neglected in the following)

$$\alpha_\mathrm{res} = \frac{\alpha}{\hat{\alpha}} \qquad \beta_\mathrm{res} = \frac{\beta - \hat{\beta}}{\hat{\alpha}} \tag{10}$$

that takes into account the estimations $\hat{\alpha}$ and $\hat{\beta}$ of the original parameters α and β. With perfect estimation the equivalent I/Q imbalance in (10) vanishes ($\alpha_\mathrm{res} = 1$ and $\beta_\mathrm{res} = 0$). For BER analysis this model has a residual gain of $\hat{\alpha}$, which has to be accounted for later in the measurements. For further details see [19].

By following this modeling approach, (2) needs to be replaced by the resulting imbalance parameters such that

$$K_{1,\mathrm{res}} = \frac{1}{2}\left(1 + \alpha_\mathrm{res} + j\beta_\mathrm{res}\right) \tag{11a}$$

$$K_{2,\mathrm{res}} = \frac{1}{2}\left(1 - \alpha_\mathrm{res} + j\beta_\mathrm{res}\right)\,. \tag{11b}$$

Consequently, the image-to-signal ratio (4) can be expressed as

$$ISR = \frac{|K_{2,\mathrm{res}}|^2}{|K_{1,\mathrm{res}}|^2} = \frac{\left(1-\alpha_\mathrm{res}\right)^2 + \beta_\mathrm{res}^2}{\left(1+\alpha_\mathrm{res}\right)^2 + \beta_\mathrm{res}^2}\,, \tag{12}$$

which can be simplified by inserting (10) to

$$ISR = \frac{(\hat{\alpha}-\alpha)^2 + \left(\hat{\beta}-\beta\right)^2}{(\hat{\alpha}+\alpha)^2 + \left(\hat{\beta}-\beta\right)^2}. \tag{13}$$

In order to minimize this ratio, or even accomplish $ISR = 0$, a minimization of the cost function

$$J\left(\hat{\alpha},\hat{\beta}\right) = (\hat{\alpha}-\alpha)^2 + \left(\hat{\beta}-\beta\right)^2 \tag{14}$$

is necessary. Hence, this satisfies the minimization of the numerator in (13). The basic idea to develop an iterative approach is the consideration that the cost function directly relates to the ISR. If two independent values of the cost function are available by fixing $\hat{\beta}$ and gaining two different settings $\hat{\alpha}_\ell$ and $\hat{\alpha}_{\ell-1}$, then

$$J\left(\hat{\alpha}_\ell,\hat{\beta}_\nu\right) - J\left(\hat{\alpha}_{\ell-1},\hat{\beta}_\nu\right) = \hat{\alpha}_\ell^2 - \hat{\alpha}_{\ell-1}^2 - 2\left(\hat{\alpha}_\ell - \hat{\alpha}_{\ell-1}\right)\alpha \tag{15}$$

holds. This equation can be rewritten to

$$\alpha = \frac{1}{2}\left[\hat{\alpha}_\ell + \hat{\alpha}_{\ell-1} - \frac{J\left(\hat{\alpha}_\ell,\hat{\beta}_\nu\right) - J\left(\hat{\alpha}_{\ell-1},\hat{\beta}_\nu\right)}{\hat{\alpha}_\ell - \hat{\alpha}_{\ell-1}}\right] \tag{16}$$

which indicates the search for α to be some kind of a bisection method. Similar considerations are possible for β. To define a relation between the cost function and the ISR, the enumerator of (14) can be approximated by $1/4\hat{\alpha}^2$ using the assumptions of realistic imbalance parameters ($\alpha \approx 1, \beta \approx 0$) and accurate estimates ($\hat{\alpha} \approx \alpha, \hat{\beta} \approx \beta$) [19]. Hence, the ISR depending on the cost function can be described as

$$ISR\left(\hat{\alpha},\hat{\beta}\right) \approx \frac{1}{4\hat{\alpha}^2}\left[(\hat{\alpha}-\alpha)^2 + \left(\hat{\beta}-\beta\right)^2\right] = \frac{1}{4\hat{\alpha}^2} J\left(\hat{\alpha},\hat{\beta}\right). \tag{17}$$

This leads to the definition of an approximated cost function $\tilde{J}\left(\hat{\alpha},\hat{\beta}\right)$ such that

$$\tilde{J}\left(\hat{\alpha},\hat{\beta}\right) = 4\hat{\alpha}^2 \cdot ISR\left(\hat{\alpha},\hat{\beta}\right). \tag{18}$$

This definition precludes the possibility to determine the imbalance parameters directly and an iterative approach is required. This bisection-like algorithm defines a method to alternately decrease the estimation error of $\hat{\alpha}$ and $\hat{\beta}$ as well as to increase the accuracy of the approximated cost function. Consequently, with the relation to the measured ISR this also leads to a decrease of the I/Q imbalance in the model (10).

For the adaptive estimation the formal function

$$p_\ell = f\left(p_{\ell-2}, p_{\ell-1}, \tilde{J}_{\ell-2}, \tilde{J}_{\ell-1}, \tau\right) \tag{19a}$$

$$= \frac{1}{2}\left[p_{\ell-2} + p_{\ell-1} - \tau \cdot \frac{\tilde{J}_{\ell-2} - \tilde{J}_{\ell-1}}{p_{\ell-2} - p_{\ell-1}}\right] \tag{19b}$$

is introduced for clear presentation, where the output p_ℓ of the function defines the updated $\hat{\alpha}$ and $\hat{\beta}$ in even or odd iterations, respectively. In this contribution, the parameter τ is introduced as a forgetting factor. With a factor $\tau < 1$ the possibility of divergence stemming from inaccurate estimates of the ISR in (18) will be decreased. A numerical analysis of the modified algorithm follows in Section III-B. A pseudo-code of the parameter adaptation with a maximum of L iterations is stated in Algorithm 1. The procedure requires initial values for the parameters in the first and second iteration for $\hat{\alpha}_1$, $\hat{\alpha}_2$ and $\hat{\beta}_1$, $\hat{\beta}_2$, respectively. They should be in the order of the expected parameters. In odd iterations updated parameters of $\hat{\alpha}$ using (19b) are obtained. Values of the cost function can always be obtained by ISR measurements and applying the approximated cost function in (18). The algorithm can be terminated after L iterations or if the ISR falls below a certain threshold. This threshold, e.g., may be defined by a fixed spectral mask.

Algorithm 1 Adaptation with modified Windisch algorithm

Require: $\hat{\alpha}_1, \hat{\alpha}_2$, $\hat{\beta}_1, \hat{\beta}_2$ and τ
1: Obtain $\tilde{J}_1, \tilde{J}_2$ with (18) using $\hat{\alpha}_1, \hat{\alpha}_2$ and $\hat{\beta}_1$
2: $\ell = \nu = 3$
3: **for** $i = 3, \ldots, L$ **do**
4: **if** $\{i$ is odd (update of $\hat{\alpha})\}$ **then**
5: $\hat{\alpha}_\ell = f\left(\hat{\alpha}_{\ell-2}, \hat{\alpha}_{\ell-1}, \tilde{J}_{i-2}, \tilde{J}_{i-1}, \tau\right)$ (cf. (19b))
6: $\ell \leftarrow \ell + 1$
7: **else** $\{i$ is even (update of $\hat{\beta})\}$
8: $\hat{\beta}_\nu = f\left(\hat{\beta}_{\nu-2}, \hat{\beta}_{\nu-1}, \tilde{J}_{i-2}, \tilde{J}_{i-1}, \tau\right)$ (cf. (19b))
9: $\nu \leftarrow \nu + 1$
10: **end if**
11: Measure ISR (cf. (4))
12: Determine $\tilde{J}_i$ (cf. (18))
13: **end for**
14: **return** $\hat{\alpha}_{\ell-1}$ and $\hat{\beta}_{\nu-1}$

B. Convergence Analysis

Considering perfect measurement of the ISR the theoretical convergence behavior of the modified Windisch algorithm can be analyzed with respect to different settings of τ. Fig. 2 shows the attainable image-to-signal ratios with initial values of $\hat{\alpha}_{1,2} = 1 \pm 0.01$ and $\hat{\beta}_{1,2} = \pm 0.01$. For this scenario I/Q imbalance parameters $g_T = 1.02$ and $\phi_T = 2^\circ$ are specified. If the ISR can be measured perfectly in the feedback path at the transmitter the original value $\tau = 1$ of the algorithm leads to the fastest convergence with a minimum ISR reached at around 15 iterations. Smaller values of τ only decrease the convergence speed, while still achieving the same minimum ISR after more iterations. Taking into account the necessary (low-resolution) A/D converters in the feedback path [19], meaning that only quantized values of the ISR are available, the measurement results are imperfect in addition to the already approximated cost function. As already mentioned in [19] the result of the algorithm strongly depends on the characteristics of the power measurement, where in this paper the setup in Section IV-B is applied. Here, noisy estimates of the quantized ISR values measured with the spectrum analyzer are obtained.

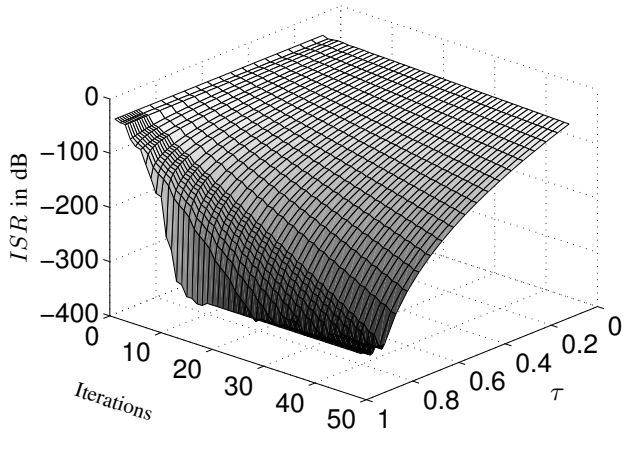

Fig. 2. Convergence of ISR with $g_T = 1.02$ and $\phi_T = 2°$ and different τ having perfect ISR measurements per iteration

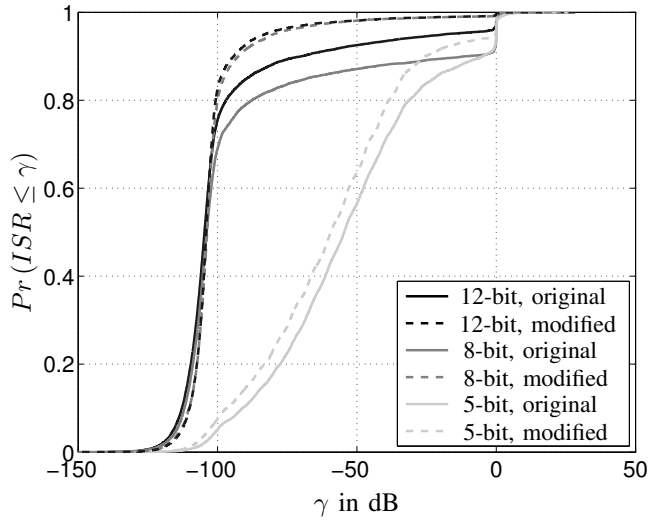

Fig. 3. Comparison of the cumulative distribution function (CDF) of the ISR after 50 iterations using the original ($\tau = 1$, $\hat{\alpha}_{1,2} = 1 \pm 0,01$, $\hat{\beta}_{1,2} = \pm 0,01$) and the modified ($\tau = 0,7$, $\hat{\alpha}_{1,2} = 1 \pm 0,05$, $\hat{\beta}_{1,2} = \pm 0,05$) Windisch algorithm with different A/D converter resolutions; I/Q imbalance parameters $g_T = 1.02$ and $\phi_T = 2°$

Considering these noisy quantized samples due to the applied hardware feedback path, the original algorithm may lead to cases of divergence. This is illustrated in Fig. 3. There, the cumulative distribution function (CDF) of the ISR obtained after 50 iterations for 10000 realizations is shown. The same parameters as in Fig. 2 are applied, where now also the modified algorithm with $\tau = 0.7$, $\hat{\alpha}_{1,2} = 1 \pm 0.05$ and $\hat{\beta}_{1,2} = \pm 0.05$ is included using dashed lines. To model the A/D converter a linear quantizer with a fixed range and a variable number of quantization bits is applied in the simulations. The results for different A/D converter resolutions indicate that the probability of a divergence can be decreased with the modified algorithm for a 5, 8 and 12-bit resolution. Especially the strong increase at around 0 dB ISR on the right side of the CDFs represent the occurrences of convergence failure. The incidence of a divergence could be effectively reduced. Therefore, the modified algorithm with the new initial values and $\tau = 0.7$ is applied in the real measurements in the next section. If complexity permits the introduction of a stopping criterion based on a maximum allowable ISR, the divergence may be avoided as there may be some values in previous iterations, which already fulfill any required spectral mask.

IV. Measurements and Results

In this section the Multiple Antenna System for ISM Band Transmission (MASI) is described. Subsequently, the estimation of the I/Q imbalance parameters of the corresponding MASI front-ends is explained in terms of the applied test setup. In the end, the BER measurement results with Tx pre-correction are shown.

A. Multiple Antenna System for ISM Band Transmission

For real system measurements an enhanced direct-conversion based multiple antenna system called MASI-2 originally presented and described in detail in [23] and firstly applied in [22] is used. With it, a verification of simulation results in a real transmission with general impairments like synchronization and timing aspects is possible. In the MASI-2 system the Tx/Rx chains are connected to a single-pole-double-throw (SPDT) switch, which allows for time duplex switching. Each Tx/Rx chain has its own front-end due to the modular architecture [23]. Now, a 2×2 transceiver system with antenna spacing $\lambda/2$ is available that can be used to investigate adaptive MIMO schemes in time division duplex (TDD) mode. The carrier frequency of the system is in the ISM band and is fixed to $f_{\mathrm{LO}} = 2.44$ GHz here, where the LO signals are provided by two external signal generators to ensure very small frequency offsets. The sampling rate is $f_s = 50$ MHz and an oversampling factor of 8 is used. The applied frame structure corresponds to the one in [22] and consists of multiple OFDM symbols with a FFT length of $N_c = 512$ before transmitting the payload. Two OFDM symbols are used for synchronisation, one is designed for channel estimation and one precoded OFDM symbol is applied for estimating the effective channel having pre-distorted pilot symbols in frequency-domain. This allows for pre-distortion in realistic scenarios with imperfect channel state information at the transmitter (CSIT) [20]. The CSIT is obtained with the reverse link estimate in TDD with the assumption of channel reciprocity. For further parameters the interested reader is referred to [22].

B. Estimation of I/Q Imbalances

Based on the iterative pre-compensation algorithm from Section III-A the inherent I/Q imbalance parameters of the MASI-2 Tx front-end modules are determined individually. Due to the parameters in the corresponding data sheets the I/Q imbalance is assumed to be small. Nevertheless, with the motivation of analyzing adaptive systems even small

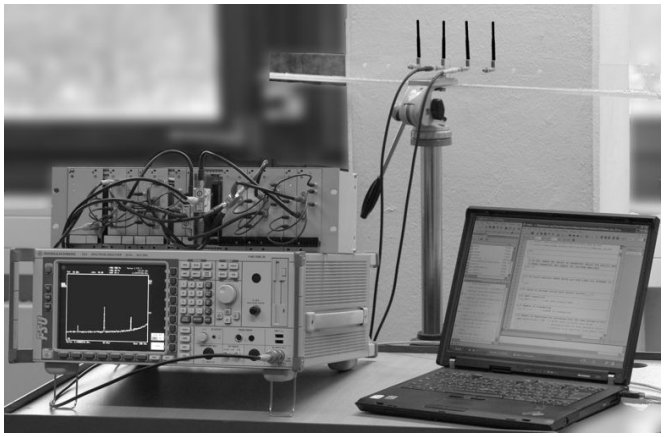

Fig. 4. Setup of the MASI I/Q imbalance measurements

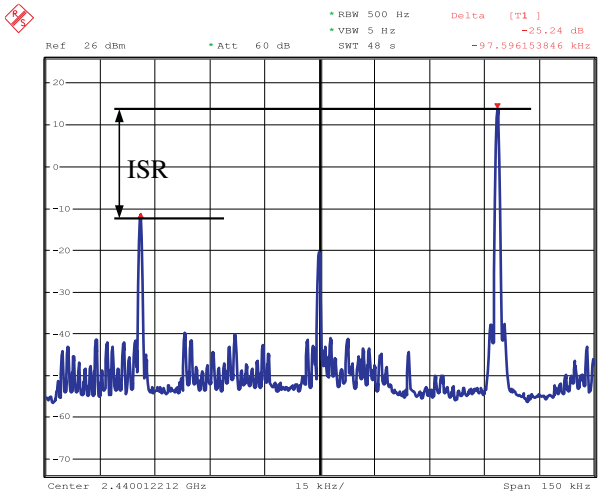

Fig. 5. Measured PSD of the MASI TxRF output of antenna port 3 using single tone low-IF mixing with I/Q mismatch

imbalances may lead to high error rates for higher order QAM modulation. As the MASI-2 system is based on the direct-conversion concept, the necessary low-IF signal must be generated to enable the ISR measurement. Therefore, only a single-tone complex exponential with frequency $f_0 = 50$ kHz is transmitted at $f_{\text{LO}} = 2.44$ GHz. Consequently, the desired signal and an image signal are excited around the carrier in the frequency domain. The resulting power density spectrum (PSD) of antenna port 3 is exemplarily shown in Fig. 5, where the right spectral line depicts the desired signal and the left spectral line denotes the image signal stemming from inherent I/Q imbalance in the transceiver. This spectrum can be further processed with the spectrum analyzer to perform the ISR measurements and to feed back the ISR value to the algorithm. The measurement setup for this procedure is shown in Fig. 4.

A more detailed block diagram of this applied scheme can be found in Fig. 6. Here, the spectrum analyzer connected via a RS232 port depicts the feedback path, which provides

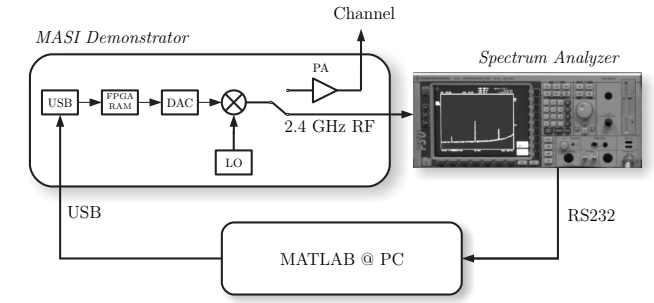

Fig. 6. Block diagram of the MASI I/Q imbalance measurement setup

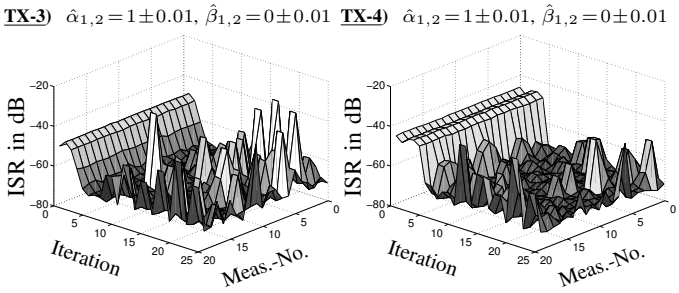

Fig. 7. ISR convergence behavior of Windisch algorithm ($\tau = 1$) in 20 measurements of MASI Tx antenna ports 3&4

noisy quantized measurements of the ISR. After calculating the updated α and β values the MASI-2 modules are pre-distorted and another measurement is conducted. Applying the compensation with the original Windisch algorithm parameters for the Tx antennas 3 and 4 several times lead to the results in Fig. 7. The minimum ISR that can be obtained with the MASI-2 system is approximately -70 dB, restricted by the maximum transmit power of 17 dBm. The convergence results show that a general convergence cannot be guaranteed with this parameter set. Here, the algorithm stops after 20 iterations. Following the analysis in Section III-B the modified algorithm with different variables τ and adjusted initial values is used in Fig. 8. On the left side the results for Tx antenna port 3 indicate that even the original algorithm achieves good convergence results while the results for antenna port 4 prove the robustness of the modified algorithm for the chosen parameters from Section III-B. There, using $\tau = 1$ results in divergence of the algorithm. Hence, the application in a real RF feedback path is not justified. To conclude, the obtained Tx I/Q imbalance parameters for the two MASI-2 transceivers are summarized in Table I. The remaining I/Q imbalance in both transceivers is relatively small with an average gain imbalance of 1% and an average phase imbalance of $0.5°$. The corresponding parameters of $\hat{\alpha}$ and $\hat{\beta}$ can be used at the transceivers to apply the pre-compensation of Tx I/Q imbalance. This is valid as long as the imbalance of the demonstrator is time-invariant, which should be a presumption for the demonstrator. In terms of the online approach with the RF feedback loop the parameters can be estimated repeatedly in pre-determined intervals.

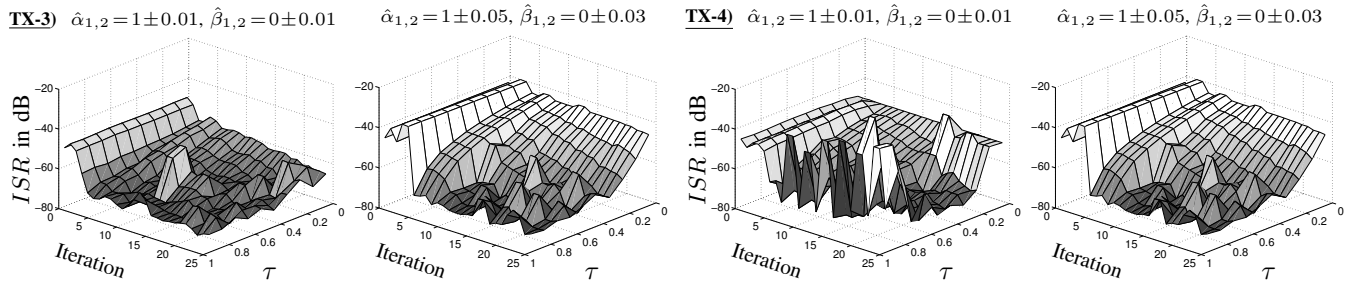

Fig. 8. Exemplary convergence behavior of the modified pre-compensation algorithm with different initial and τ values for the MASI transmit antenna front-ends

TABLE I
ESTIMATED I/Q IMBALANCE PARAMETERS OF MASI-2 TX ANTENNA PORTS AFTER 20 ITERATIONS WITH $\tau = 0.7$

Tx port	$\hat{\alpha} \mid g_{T,n_B}$	$\hat{\beta}$	ϕ_{T,n_B}
1	1.010	$3 \cdot 10^{-3}$	$0.17°$
2	0.990	$1 \cdot 10^{-2}$	$0.58°$
3	1.008	$2.5 \cdot 10^{-3}$	$0.15°$
4	0.991	$9 \cdot 10^{-3}$	$0.52°$

C. Performance Results

For the measurements of adaptive multi-antenna OFDM scenarios with the investigated I/Q pre-compensation the described MASI-2 system is used. The two transceivers are located in two neighboring offices separated by a distance of around $5m$ with no direct line-of-sight. To obtain bit error rates (BER) versus receive symbol-to-noise ratios (Rx SNR), the Rx SNR is modeled by adding extra white Gaussian noise to the receive signal at symbol rate. The corresponding noise variances of the different receive symbol-to-noise ratios are calculated and scaled depending on the measured receive symbol power.

Fig. 9 depicts the BER vs. Rx SNR curves for the uncoded point-to-point communication scenario described in Case I in Section II-B with and without I/Q imbalance pre-compensation. The spectral efficiency is set to $\eta = 2$ bit/s/Hz and the loading algorithm of Krongold in [5] is applied. The results indicate an improved performance, which can be achieved by pre-compensating the I/Q imbalances at the transmitter side. Although the gain is at most 1 dB in this scenario it shows the possible performance improvement especially if the spectral efficiency would be increased [7]. The same setup was simulated and measured for a multi-user multiple-input single-output (MU-MISO) OFDM system with zero-forcing pre-equalization as stated in Case II in Section II-B. Therefore, the receive antennas are processed independently at the second transceiver, whereas the antenna spacing remains $\lambda/2 \approx 6$ cm in this scenario. Fig. 10 depicts the results for this point-to-multipoint system and an increased spectral efficiency of $\eta = 4$ bit/s/Hz, again with uncompensated I/Q imbalance and after pre-distortion. The higher spectral efficiency was chosen to obtain higher order modulation. In the previous case this was achieved by the application of the bit loading algorithm. Similarly, the BER performance is increased with a gain of approximately 2 dB at a BER of 10^{-2} for the compensated case. Of course, the application of channel coding will diminish the gain in these cases. Nevertheless, this measurement results indicate the applicability of the pre-compensation algorithm in real scenarios. The effort that must be spent for I/Q imbalance correction depends on the modulation alphabet size, which is continuously increasing in modern wireless transmission schemes.

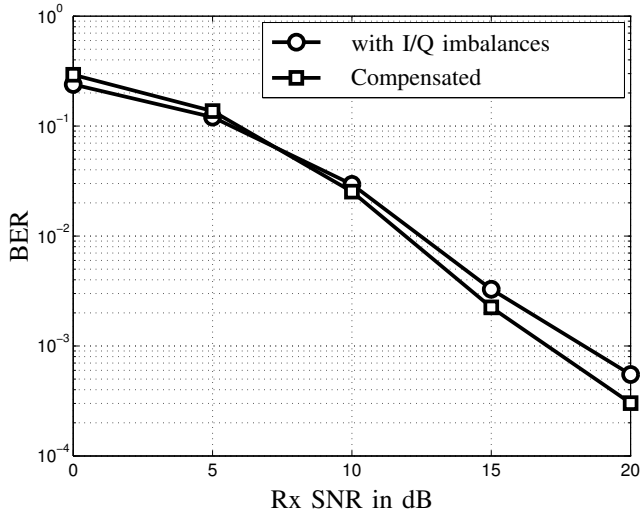

Fig. 9. Measured bit error rate versus receive SNR for the MASI MIMO-OFDM system with $N_B = N_M = 2$, $N_C = 512$ subcarriers and $\eta = 2$ bit/s/Hz for scenarios with I/Q imbalances and after applying the compensation algorithm

V. CONCLUSION

In this paper the application of an (on-line) iterative I/Q imbalance pre-compensation algorithm was investigated with a multi-antenna hardware demonstrator transmitting in the ISM-band. Corresponding off-line single-tone measurement results in the (virtual) low-IF feedback path at the transmitter showed an almost perfectly suppressed image signal. For robustness of the algorithm a forgetting factor τ is introduced to improve the convergence behavior if quantization errors coming from the A/D converter in the feedback path are existent. The subsequent compensation based on the estimated I/Q imbalance parameters improved the BER performance in an uncoded scenario and achieved the same gains as if

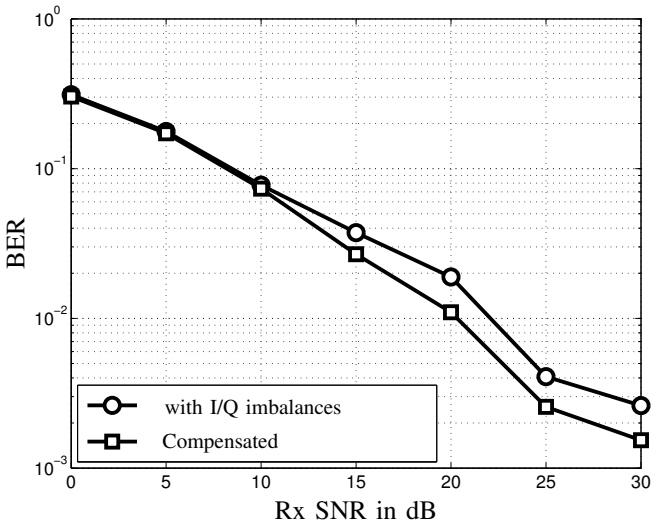

Fig. 10. Measured bit error rate versus SNR for the MASI MU-MISO-OFDM system with $N_B = N_M = 2$, $N_C = 512$ subcarriers and $\eta = 4$ bit/s/Hz for scenarios with I/Q imbalances and after applying the compensation algorithm

hardware calibration would have been executed. The gains are smaller than expected, which is due to the quality of the hardware components in the demonstrator. Nevertheless, the compensated system is robust to deal with higher order modulation in upcoming wireless OFDM systems due to reduced ICI. In addition, the application of cheaper front-end modules is offered if the RF feedback loop can also be designed with low costs. Furthermore, applications with low-IF transceivers will also benefit from an image signal suppression to fulfill spectral mask constraints.

ACKNOWLEDGEMENTS

The authors like to thank C. Bockelmann, H. Paul and H. Masemann for the fruitful discussions and their support throughout the measurement campaign.

REFERENCES

[1] F. Horlin and A. Bourdoux, *Digital Compensation for Analog Front-Ends - A New Approach to Wireless Transceiver Design*, John Wiley & Sons, 2008.

[2] G. Fettweis, M. Löhning, D. Petrovic, M. Windisch, P. Zillmann, and W. Rave, "Dirty RF: A New Paradigm," *International Journal of Wireless Information Networks (IJWIN)*, vol. 14, no. 2, pp. 133–148, June 2007.

[3] L. Brötje, *Fehlereinflüsse in direktmischenden Strukuren zur OFDM-Übertragung (in German)*, Ph.D. thesis, University of Bremen, Germany, Dec. 2004.

[4] T. C. W. Schenk, *RF Impairments in Multiple Antenna OFDM*, Ph.D. thesis, Technical University Eindhoven, Netherlands, Nov. 2006.

[5] B. S. Krongold, K. Ramchandran, and D. L. Jones, "Computationally Efficient Optimal Power Allocation Algorithms for Multicarrier Communication Systems," *IEEE Transactions on Communications*, vol. 48, no. 1, pp. 23–27, Jan. 2000.

[6] M. Joham, K. Kusume, M. Gzara, W. Utschick, and J. A. Nossek, "Transmit Wiener Filter for the Downlink of TDD DS-CDMA Systems," in *Proc. IEEE Int. Symp. on Spread Spectrum Techniques and Applications (ISSSTA)*, Prague, Czech Rep., Sept. 2002, vol. 1.

[7] M. Niemiec, "Sendeseitige Korrektur von I/Q-Unsymmetrien bei adaptiven MIMO-OFDM Systemen (in German)," Diploma Thesis, University of Bremen, Germany, Oct. 2009.

[8] R. Marchesani, "Digital Precompensation of Imperfections in Quadrature Modulators," *IEEE Transactions on Communications*, vol. 48, no. 4, pp. 552–556, Apr. 2000.

[9] M. Windisch, *Estimation and Compensation of I/Q Imbalance in Broadband Communications Receivers*, Ph.D. thesis, Technical University Dresden, Germany, Mar. 2007.

[10] J. K. Cavers and M. W. Liao, "Adaptive Compensation for Imbalance and Offset Losses in Direct Conversion Transceivers," *IEEE Transactions on Vehicular Technology*, vol. 42, no. 4, pp. 581–588, Nov. 1993.

[11] M. Faulkner, T. Mattsson, and W. Yates, "Automatic Adjustment of Quadrature Modulators," *IEEE Electronic Letters*, vol. 27, no. 3, pp. 214–216, Jan. 1991.

[12] G. Yang, G. Vos, and H. Cho, "I/Q Modulator Image Rejection Through Modulation Pre-Distortion," in *IEEE Vehicular Technology Conference (VTC 96)*, Atlanta, GA, USA, Apr. 1996.

[13] X. Huang and M. Caron, "Gain/Phase Imbalance and DC Offset Compensation in Quadrature Modulators," in *IEEE Intl. Symposium on Circuits and Systems (ISCAS 02)*, Scottsdale, AZ, USA, May 2002.

[14] Z. Zhu and X. Huang, "Adaptive Compensation of Gain/Phase Imbalances and DC-Offsets Using Constant Modulus Algorithm," in *IEEE International Conference on Acoustics, Speech, and Signal Processing (ICASSP)*, Montreal, Canada, May 2004.

[15] T. C. W. Schenk, P. F. M. Smulders, and E. R. Fledderus, "Estimation and Compensation of Frequency Selective TX/RX IQ Imbalance in MIMO OFDM Systems," in *IEEE International Conference on Communications (ICC)*, Istanbul, Turkey, June 2006.

[16] T. C. W. Schenk, P. F. M. Smulders, and E. R. Fledderus, "Estimation and Compensation of TX and RX IQ Imbalance in OFDM Based MIMO Systems," in *IEEE Radio and Wireless Symposium (RWS 06)*, San Diego, CA, USA, Jan. 2006.

[17] J. Tubbax, B. Come, L. Van der Perre, S. Donnay, M. Moonen, and H. De Man, "Compensation of Transmitter IQ Imbalance for OFDM Systems," in *IEEE International Conference on Acoustics, Speech, and Signal Processing (ICASSP)*, Montreal, Canada, May 2004.

[18] M. Windisch, "Transmitter and transmission method," EU Patent Application 04360087.3, Sept. 2004.

[19] M. Windisch and G. Fettweis, "Adaptive I/Q Imbalance Compensation in Low-IF Transmitter Architectures," in *IEEE Vehicular Technology Conference Fall (VTC)*, Los Angeles, CA, USA, Sept. 2004.

[20] H. Busche, A. Vanaev, and H. Rohling, "SVD-based MIMO Precoding and Equalization Schemes for Realistic Channel Knowledge: Design Criteria and Performance Evaluation," *Wireless Personal Communications - An International Journal*, vol. 48, no. 3, pp. 347–359, June 2008.

[21] T. C. W. Schenk, *RF Imperfections in High-rate Wireless Systems: Impact and Digital Compensation*, Springer Netherlands, 2008.

[22] M. Stefer, M. Petermann, M. Schneider, D. Wübben, and K.-D. Kammeyer, "Influence of Non-reciprocal Transceivers at 2.4 GHz in Adaptive MIMO-OFDM Systems," in *14th International OFDM-Workshop (InOWo 09)*, Hamburg, Germany, Sept. 2009.

[23] J. Rinas, R. Seeger, L. Brötje, S. Vogeler, T. Haase, and K.-D. Kammeyer, "A Multiple-Antenna System for ISM-Band Transmission," *EURASIP Journal on Applied Signal Processing - Special Issue on Advances in Smart Antennas*, vol. 2004, no. 9, pp. 1407–1419, Aug. 2004.